Asymmetric response of superconducting niobium-tunnel-junction x-ray detectors

M. Ohkubo*
Forschungszentrum Karlsruhe, Institut für Nukleare Festkörperphysik, Postfach 3640, D-76021, Karlsruhe, Germany

J. Martin, K. Drachsler, R. Gross,† and R. P. Huebener
Physikalisches Institut, Lehrstuhl Experimentalphysik II, Universität Tübingen, Morgenstelle 14, D-72076 Tübingen, Germany

I. Sakamoto and N. Hayashi
Electrotechnical Laboratory, Umezono, Tsukuba, Ibaraki, 305, Japan
(Received 19 April 1996; revised manuscript received 14 June 1996)

The asymmetric response of the counter and base electrodes of x-ray detectors employing polycrystalline niobium tunnel junctions has been studied by low-temperature scanning electron microscopy (LTSEM). LTSEM has revealed that the base electrode produces a signal more than two times larger than the counter electrode, and effective quasiparticle lifetimes are 100 ns in the counter and 280 ns in the base. Based on the I-V characteristics and the measured effective quasiparticle lifetimes, we propose a model structure for a spatial variation of the gap parameter Δ, which involves proximity quasiparticle trapping layers. The small counter signal is caused by the shorter quasiparticle lifetime and the trapping effect. The LTSEM results are consistent with x-ray spectra for a radioactive ^{55}Fe source. [S0163-1829(96)06437-5]

I. INTRODUCTION

Superconducting tunnel junctions (STJ's) have been extensively studied for a promising application to high-energy-resolution x-ray detectors in a range of 1–10 keV. An x-ray photon deposited in either superconducting electrode of a superconductor-insulator-superconductor (SIS) junction breaks Cooper pairs and creates quasiparticles in excess of a thermal equilibrium density. Those quasiparticles can be measured through quasiparticle tunneling of SIS junctions operated on Giaever mode. High energy resolution is envisaged from a small superconducting-energy gap 2Δ that is more than 1000 times smaller than that of silicon. The intrinsic resolution of STJ detectors is given by $\Delta E/E = 2\sqrt{\ln 4}(F\varepsilon/E)^{1/2}$ in full width at half maximum (FWHM), where E is the radiation energy, F is the Fano factor, and ε is the mean energy necessary to create one quasiparticle. Theoretical predictions have indicated that $F \cong 0.2$ and $\varepsilon \cong 1.7\Delta (= 2.64$ meV for niobium)[1,2] and thus an intrinsic energy resolution of 0.07% (4 eV for the 6-keV x rays). However, no experimental results have realized this value because of tunneling barrier imperfections, electric noises, and quasiparticle losses. In niobium junctions, the best resolutions are in a range of 53–88 eV for the 6-keV x rays,[3–5] and a resolution of 29 eV has been achieved with aluminum quasiparticle-trapping layers.[6]

Photoabsorption in the superconducting electrodes induces several processes. The processes have been described in literature.[2,7,8] Here we mention them briefly. In niobium the photoabsorption of the 6-keV x ray creates a photoelectron with an energy of E-E_L (3.2–3.5 keV), where E_L is the binding energy of the L shell. The L-shell vacancy causes an Auger electron emission at 2.5 keV, which is dominant at a probability of more than 96%, or a radiative M-L transition. These electrons lose their energies through ionizations and multiple scattering, which finally create quasiparticles. The quasiparticles relax to energies just above 2Δ within 10^{-12}–10^{-9} s after the photoabsorption, and then recombine into Cooper pairs.[8] In order to obtain a reasonable signal, the excess quasiparticles should be counted within a quasiparticle lifetime. Hence, an important issue of the high energy-resolution detectors is to obtain a long quasiparticle lifetime and a short tunneling time. The effective quasiparticle lifetime is longer than the intrinsic lifetime because a quasiparticle recombination creates a phonon with an energy of $\geqslant 2\Delta$ that breaks a Cooper pair again.[9,10] Thus the phonon loss time plays an important role. On the other hand, the tunneling time is basically determined by an electrode thickness and a normal-state junction resistance, which is a measure of tunneling barrier transparency.[11]

It is known that two electrodes of STJ detectors generally produce an asymmetric response, which appears as double peaks to monochromatic x rays on pulse height spectra,[12] although there is a report on polycrystalline niobium junctions of which the response seems to be symmetric.[13] The asymmetric response has been reported in polycrystalline tin or niobium junctions.[5,14,15] Recently, niobium junctions have been frequently employed, because a combination of niobium and aluminum enables one to fabricate high-quality tunnel junctions.[16] In any case, there is no consensus on which electrode makes a larger signal. This may be understood by taking into account phonon escape processes from junctions into surroundings. However, an exact evaluation of phonon escape times seems impossible. Contrarily, in niobium junctions with single-crystalline base electrodes it has been consistently reported that the single-crystalline bases produce considerably higher signals than the polycrystalline counters.[3,17,18] The larger base signals may primarily result from longer quasiparticle lifetimes in single-crystalline niobium. It has been also implied that a contaminated surface layer and photoelectron escape cause the poor counter-performance.[19–21] However, the properties of counter or base

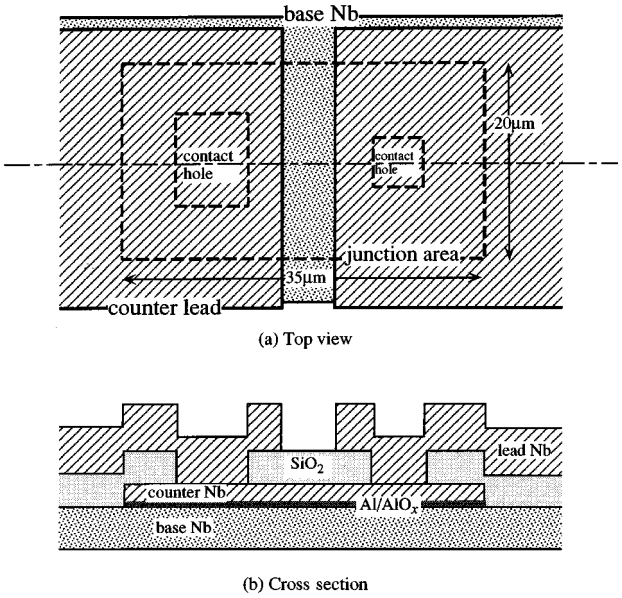

FIG. 1. Top view and cross section of the niobium junction on a Si wafer covered by a 20-nm thick MgO layer. The film thicknesses are 200 nm (base Nb), 10 nm (Al/AlO_x), 100 nm (counter Nb), 300 nm (SiO_2), and 400 nm (lead Nb).

electrodes have not been measured separately, and thus the cause of the asymmetric response is obscure.

Recently, it has been pointed out with low-temperature scanning electron microscopy (LTSEM) that the single-crystalline niobium base produces a signal 2–3 times larger than the polycrystalline counter,[18] and additionally the base signal of a polycrystalline niobium junction is larger than the counter one.[22] These results were obtainable through an accurate controllability of the position and depth of small perturbation in LTSEM. In this study, we have also employed LTSEM to determine explicitly which electrode of our polycrystalline niobium junctions produces a larger signal and to measure quasiparticle lifetimes separately. LTSEM data are analyzed in combination with I-V characteristics and x-ray spectra in detail. Finally, a model structure for a spatial variation of the gap parameter is proposed to explain observed asymmetric response.

II. EXPERIMENT

The niobium junctions were fabricated by conventional photolithographic and reactive ion etching techniques. The structure of the junctions is shown in Fig. 1. A typical junction on the wafer had a critical current density of $j_c=120$ A/cm^2, a normal-state specific resistance of $\rho_n=16\ \mu\Omega\ \mathrm{cm}^2$. The I-V characteristic curve measured at 4.2 K is shown in Fig. 2. The sum of the gap parameters is 2.86 meV at 4.2 K. A small knee at 0.15 mV is assigned to a singularity at the gap parameter difference between the counter and base, $eV=\Delta_c-\Delta_b$. It is thus evaluated that the gap parameters at 0 K are $\Delta_c(0)=1.55$ meV, which is equal to the bulk value, and $\Delta_b(0)=1.40$ meV, which is suppressed by the proximity effect in the aluminum layer. It is expected that the base niobium layer underneath the proximity layer has the same gap as Δ_c. The Δ reduction of 0.15 meV due to the Al layer ($\sim$8 nm) agrees well with dependence of Δ on aluminum

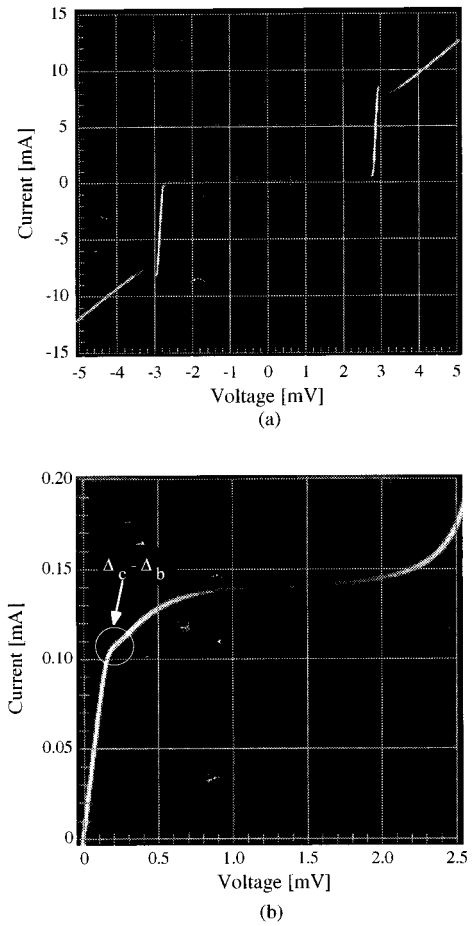

FIG. 2. I-V characteristic curve at 4.2 K: (a) a wide voltage scan and (b) a magnified curve in the subgap region.

thicknesses.[23] The above interpretation is compatible with that in Ref. 24.

A junction of $35\times20\ \mu\mathrm{m}^2$ was analyzed by LTSEM. Details about LTSEM have been published elsewhere.[25,26] Throughout the measurements the dc Josephson current was suppressed by applying a magnetic field parallel to the junction surface. The junction was kept at 2.0 K by pumping ^{4}He, and biased at 0.6 mV with a current bias network. Two kinds of measurements were performed: spatially resolved measurement (two-dimensional image) and time-resolved measurement (time decay). Two-dimensional images of junction response were recorded with long electron pulses for 25 μs at different energies between 5 and 15 keV. The measured signal reflects the steady-state density of the excess quasiparticles, since the pulse duration is exceedingly longer than quasiparticle lifetimes. We observed no nonlinear dependence of the junction response on electron-beam currents in a range of 2–8 pA. Hence, the perturbation is considered to be small. Time decay curves were measured with short pulses for 100 ns at 10 keV which contain 19 electrons, in order to evaluate the quasiparticle lifetimes.

X-ray measurements were performed in a ^{3}He cryostat at 0.4 K. The whole area of a junction of $50\times80\ \mu\mathrm{m}^2$ on the same wafer was uniformly irradiated with a radioactive ^{55}Fe source, which emits the Mn $K\alpha$ 5.89 keV (88%) and Mn $K\beta$ 6.49 keV (12%) characteristic x rays. The junction was biased at voltages between 0.13 and 0.6 mV with a constant

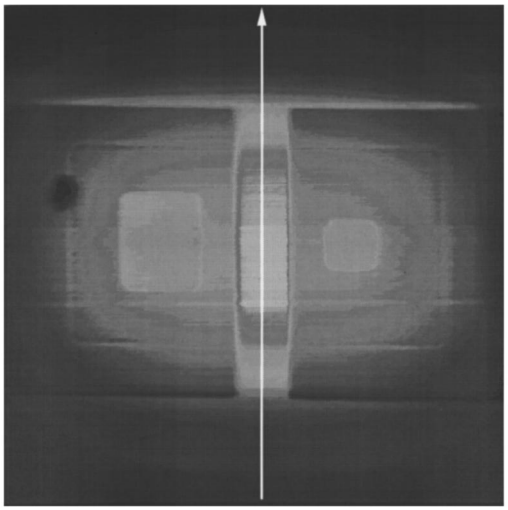

FIG. 3. Two-dimensional LTSEM image of the junction response to the 15 keV electrons. The signal heights are toned from black for the lowest signal to white for the highest one. The corresponding top view is shown in Fig. 1. The arrow indicates the direction of the line scan in Fig. 4.

current source. In the bias point range the dynamic specific resistance is 0.05 Ω cm^2. Readout electronics were a conventional combination of a preamplifier, a shaping amplifier, an analog-to-digital converter, and a multichannel analyzer.

III. EXPERIMENTAL RESULTS AND DISCUSSION

A. Two-dimensional image of junction response

Figure 3 shows the two-dimensional image of the junction response to the 15 keV electrons. The 15-keV electrons pass through most parts of the junction structure, and thus the junction area and the contact holes are visible. The line scan at 5 keV along the vertical arrow is shown in Fig. 4. From the electron ranges of 120 nm in niobium and 380 nm in SiO_2 at 5 keV,[27] it is obvious that the electrons are completely stopped within the counter niobium in the junction area and within the base niobium in the base area where no counter and barrier are present. Thus, the equal energies were deposited in either electrode. The signal curve is almost flat in the junction area. On the other hand, in the base area the signal exhibits a maximum just outside the junction area and rapidly decreases toward the base edge. The step just outside the junction area indicates that the base produces a signal more than two times larger than the counter. The value two is considered to be a lower limit of the signal height ratio, because the signal from the base area reflects the number of quaisparticles that diffuse into the junction area and at least half of the quasiparticles in the base cannot be counted when the electron beam irradiates just outside the junction area. Thus, the intrinsic signal height ratio may be close to four.

B. X-ray spectra

The present junction structure has not been optimized for x-ray spectroscopy. Nevertheless, the junction successfully produces the clear x-ray peaks on the pulse height spectrum shown in Fig. 5. Two peaks are apparently recognized with a

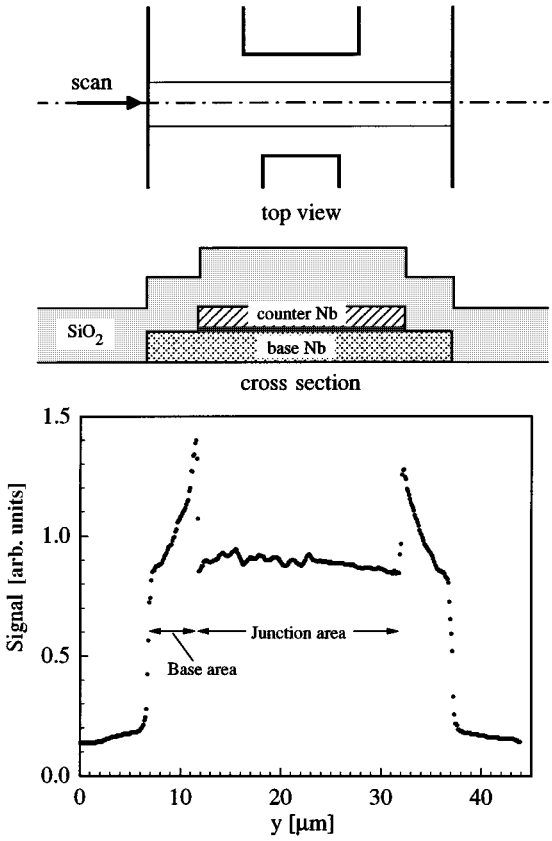

FIG. 4. Line scan of the LTSEM image at 5 keV and junction structure along the arrow indicated in Fig. 3. The junction signal is plotted against the electron-beam coordinate.

low-energy background, and the higher peak is accompanied by a shoulder. In consideration of the above LTSEM results, the higher and lower peaks are assigned to the absorptions of the Mn $K\alpha$ line in the base and counter, respectively. The shoulder is due to the absorption of the Mn $K\beta$ line in the base. Concerning the counter, these two lines produce the single peak due to a lower energy resolution.

The signal height ratio of the base and counter peaks is two, which coincides with the lower limit of the LTSEM

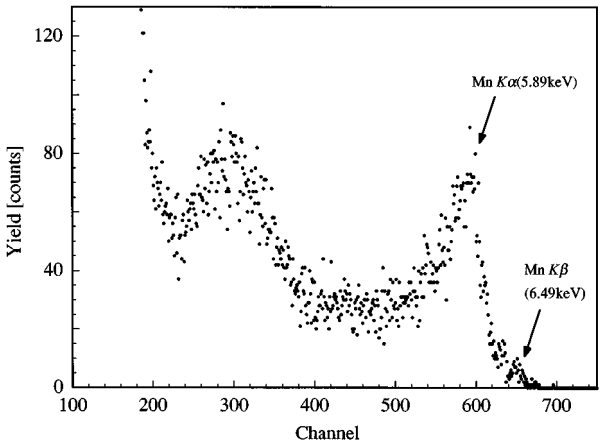

FIG. 5. X-ray spectrum for a ^{55}Fe source at a bias voltage of 0.25 mV and 0.4 K. The higher and lower peaks are assigned to the x-ray events in the base and counter electrodes, respectively. The signal of the Mn $K\beta$ line appears as a shoulder of the higher peak.

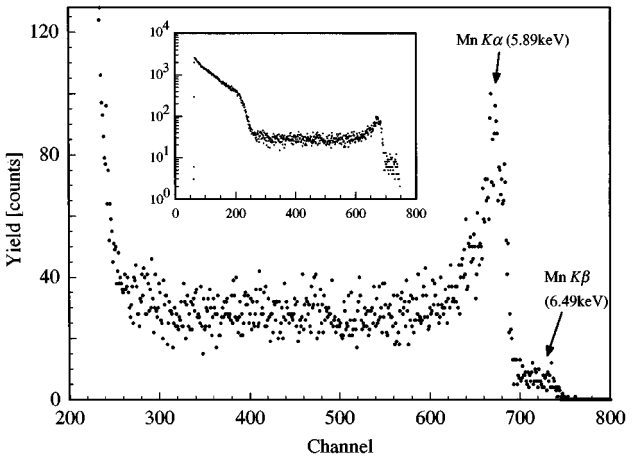

FIG. 6. X-ray spectrum measured at a bias voltage of 0.4 mV and 0.4 K. The inset displays the same spectrum with the log scale. The energy resolution for the Mn $K\alpha$ is 300 eV in FWHM. The Mn $K\beta$ line is moderately separated because of a better energy resolution than in Fig. 5. The low-energy background below the 250th channel is caused by the x-ray events in the leads far from the junction area or the substrate events.

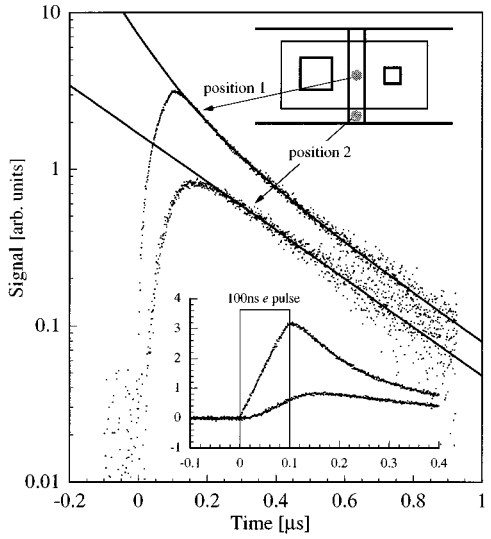

FIG. 7. Time decay curves measured with the 10-keV electron pulse for 100 ns at different two positions. The solid lines show the numerical fit results. It is evaluated that the quasiparticle lifetimes are 100 ns in the counter and 280 ns in the base electrodes. In the inset the curves are plotted with the linear scale.

result accidentally. However, the x-ray and LTSEM experiments were performed at the different bias points and temperatures. In addition, the x rays irradiate the whole area, while the electrons stimulate the certain positions. Thus, we cannot exactly compare the two results. Nevertheless, at the same bias point as the LTSEM measurements, only a single set of peaks was observed similarly to Fig. 6. The signal from the counter was considered to be obscure on the large yield from the low-energy background, which means that the signal height ratio is more than two. Hence, the two results of the x-ray and LTSEM measurements are consistent.

The best energy resolution is obtained at a bias point of 0.4 mV, as shown in Fig. 6. The energy resolution for the Mn $K\alpha$ line is 300 eV in FWHM, and the Mn $K\beta$ line is comparatively well separated from the $K\alpha$ line.

C. Time decay: quasiparticle lifetimes

The time decay curves of the junction response to the 10-keV pulse for 100 ns are shown in Fig. 7. As displayed in the inset concerning the linear scale plot, the signal rises during the electron pulse are linear. This ensures that the perturbation is small or the self-recombination is negligible. At position 1 the signal reaches a maximum just at the end of the electron pulse, while at position 2 it is delayed by about 50 ns. This delay is consistent with a time necessary for the quasiparticles created in the base area to reach the junction area, namely a mean diffusion length $\sqrt{2Dt}$ for 50 ns is an order of the base area width.[28] Numerical fits with a two-exponential-term formula were performed with a nonlinear optimization method. The best fits for the decay curves are expressed by $1.59\exp(-t/0.103)+1.95\exp(-t/0.279)$ at position 1 and $1.19\exp(-t/0.281)$ at position 2, where t is the time after the pulse end in an unit of μs. At position 1 the 10-keV electrons stimulate both the counter and base, while at position 2 the electrons stimulate only the base. It is thus demonstrated that the quasiparticle lifetimes are 100 ns in the counter and 280 ns in the base.

In literature measured effective lifetimes in niobium are strongly dependent upon experimental conditions. That ranges, for example, from 40 ns in a double tunnel junction device to 50 μs in a high purity bulk single crystal.[29,30] The present effective lifetimes, which are remarkably shorter than that of the bulk single crystal, may be related to a fast phonon loss at grain boundaries. There are two phonon loss processes in general: phonon escape into surroundings and bulk phonon decay into energies below 2Δ. The phonon escape occurs only near a junction-substrate interface within a phonon pair-breaking mean free path Λ, while the bulk phonon decay can occur everywhere in the electrodes. In niobium junctions the phonon escape has generally been considered to be a major phonon loss process in literature. However, it has been pointed out that even in a 100 nm thick niobium film the phonon escape to surroundings is negligible, since the Λ of niobium is exceptionally smaller than those for other elemental superconductors.[31,32] Hence, the bulk phonon decay should be dominant in niobium. As a result, in our junctions the effective quasiparticle lifetime τ_r^* is expressed by

$$\tau_r^* = \tau_r(1+\tau_\gamma/\tau_B), \tag{1}$$

where τ_r is the intrinsic lifetime, τ_γ is the phonon decay time, and τ_B is the phonon pair-breaking time. The intrinsic lifetime calculated by a low-temperature approximation is $\tau_r=50$ ns at 2.0 K and τ_B equals 1.9 ps.[9,31] The phonon decay time is thus estimated at $\tau_\gamma=10$ ps by taking the measured lifetime of the base. In a bulk single-crystalline niobium it has been reported that the phonon decay time at an energy of 2Δ(Al) is 145 μs that is a factor of 100 shorter than a theoretical anharmonic decay time.[30] It was envisaged that the surface of the bulk niobium caused a fast phonon decay. When we take a relation of $\tau_\gamma \propto E^{-5}$ for the anharmonic decay,[33] the phonon decay time at 2Δ(Nb) is an order of 10^{-5} s, which is still longer than 10 ps. It is well known

that the polycrystalline niobium films have a columnar structure with grain sizes of 30–80 nm.[34,35] The columnar structure can cause phonon inelastic scattering within τ_B in consideration of the Λ. It is therefore reasonable that the effective lifetimes are shortened by the fast phonon decay enhanced at the grain boundaries.

The quasiparticle lifetimes significantly influence the signal height of junction response, which is directly related to the collected excess charge Q. The Q is expressed by

$$Q = Q_0 \frac{\tau_{\rm tun}^{-1}}{\tau_{\rm tun}^{-1} + \tau_r^{*-1}}, \tag{2}$$

where Q_0 is the total charge of the excited quasiparticle, and $\tau_{\rm tun}$ is the quasiparticle tunneling time.[2] Equation (2) is valid if there is no back tunneling, the so-called Gray effect.[36] In our junction the signal amplification due to the Gray effect is negligible, since the measured effective lifetimes are shorter than the tunneling times. The tunneling time in $kT \ll eV_B < 2\Delta$, where V_B is the bias voltage, for junctions with two identical electrodes is expressed by

$$\tau_{\rm tun} = 4e^2 \rho_n N(0) d \frac{\sqrt{(\Delta + eV_B)^2 - \Delta^2}}{\Delta + eV_B}, \tag{3}$$

where $N(0)$ is the single spin density of states at the Fermi energy, and d is the thickness of the electrode from which quasiparticles tunnel to the other electrode.[11] In the present junction there is the proximity layer under the barrier in the base. Nevertheless, since the Δ reduction is small and the bias voltage sufficiently exceeds $(\Delta_c - \Delta_b)/e$, the tunneling times can be well approximated by Eq. (3). Equation (3) is valid for both tunneling processes of counter-to-base and base-to-counter independently of the bias polarity.[11] The tunneling times are expected to be 2.3 μs for the counter-to-base tunneling and 4.5 μs for the base-to-counter tunneling. From Eq. (2) the ratio of the collected charge from the base Q_b to that from the counter Q_c is estimated at $Q_b/Q_c = 1.4$ by using the measured lifetimes. The value is less than the measured lower limit of the signal height ratio.

It is known that the proximity layer with a reduced Δ acts as a quasiparticle trapping layer and enhances tunneling rates.[37–39] Quasiparticle lifetimes and tunneling times in Nb-Al proximity junctions have been calculated theoretically.[40] Although the theory cannot be simply applied to the present case of the condition of $k_BT > (\Delta_c - \Delta_b)$ at 2.0 K, it is predicted that a lower limit of $\tau_{\rm tun}$ for base-to-counter is 3 μs in consideration of the trapping effect due to the Al layer in the base. Accordingly, the upper limit of the predicted signal ratio is two at 2.0 K. That value is still inconsistent with the measured signal height ratio, which indicates that no significant trapping effect of the Al proximity layer is expected. Thus, another cause of the smaller counter signal should be considered.

IV. INTERPRETATION OF THE ASYMMETRIC RESPONSE

In order to explain the unexpected large asymmetric response, we introduce a simple model structure illustrated in Fig. 8. In addition to the aluminum proximity layer $R3$ in the base, let us assume that there is another region $R1$ with a reduced Δ in the counter. The other regions, $R2$ and $R4$, have the same gap parameter of 1.55 meV.

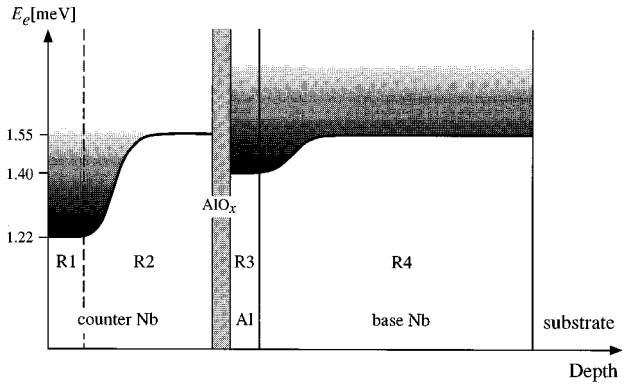

FIG. 8. Model structure of the gap parameter variation, which is derived from the I-V characteristics and the measured quasiparticle lifetimes. The solid line shows the gap parameter variation, and the shadow represents the distribution of electron quasiparticles at $T \neq 0$. The scales of both axes are inaccurate.

We estimate the Δ value in $R1$ from the measured quasiparticle lifetimes. Since the phonon decay times in both electrodes are supposed to be the same, the ratio of the effective lifetime in the counter to that in the base equals the ratio of the intrinsic lifetimes. The τ_r is given by

$$\tau_r^{-1} = \frac{2\pi\alpha^2 F}{\hbar Z_1(0)} \frac{N_{\rm th}}{N(0)}, \tag{4}$$

where $\alpha^2 F$ is the product of the electron-phonon coupling strength and the density of phonon states, and $Z_1(0)$ is the electron-phonon coupling renormalization factor.[9] If we take a low-frequency approximation of $\alpha^2(\Omega)F(\Omega) = b\Omega^2$, where Ω is the phonon energy and is supposed to be equal to 2Δ, and $N_{\rm th} = 2N(0)\Delta(\pi k_B T/2\Delta)^{1/2}\exp(-\Delta/k_BT)$, Eq. (4) is rewritten by

$$\tau_r^{-1} = \frac{16\pi b}{\hbar Z_1(0)} \sqrt{\frac{\pi k_B T}{2\Delta}}\, \Delta^3 \exp\left(-\frac{\Delta}{k_B T}\right). \tag{5}$$

The values of b and $Z_1(0)$ are tabulated in Ref. 9. When a single set of the b and Z_1 values is assumed for the present junction, the ratio of the lifetimes in the counter and base is given by

$$\frac{\tau_{r,c}^*}{\tau_{r,b}^*} = \frac{\tau_{r,c}}{\tau_{r,b}} = \left(\frac{\Delta_c}{\Delta_b}\right)^{-5/2} \exp\left(\frac{\Delta_c(0) - \Delta_b(0)}{k_B T}\right). \tag{6}$$

By employing the measured lifetime ratio and an average gap value of 1.48 meV for the base, it is calculated that $\Delta_c = 1.22$ meV. This large Δ reduction more than the thermal energy enables us to replace Δ_c by Δ_{R1}, which means that most of the quasiparticles are confined in $R1$. In other words, the lifetime in $R1$ is shorter than that in the base predominantly because of a larger number of the thermal quasiparticles that originates from the small Δ. The estimated Δ value of 1.22 meV in $R1$ is an effective value, since the values of b and Z_1 in the proximity layer are unknown.

A question is what the reduced-Δ region is in the counter. It is well known that the surface of niobium is easily oxidized in air, and such niobium oxides as Nb_2O_5 and NbO_x,

and Nb-O solid solutions are formed even at room temperature.[20] Moreover, the presence of a normal-metal layer underneath a niobium-oxide layer has been proposed in Nb-NbO_x-superconductor junctions.[41] Nb_2O_5 is an insulator, while NbO_x is usually a normal metal. The Nb-O solid solutions are superconductors of which T_c is reduced by 0.93 K/O at. %.[42,43] The formation of these phases on niobium surfaces has been confirmed by Rutherford backscattering, x-ray photoemission spectroscopy, and other methods.[20,44] In the present junctions, the niobium surface was exposed in air during the fabrication processes and even the wafer was occasionally heated up at about 100 °C in air for ~30 min before the SiO_2 deposition, and thus the oxide formation on the counter surface is highly expected. The contribution of a low-T_c layer of the Nb-O solid solutions is unlikely, because the solubility limit of oxygen is expected to be less than 1 at. % even at 600 °C, which corresponds to a negligible reduction of T_c or Δ.[45] Hence, it is most probable that a NbO_x metal layer is present near the counter surface, and functions as a strong trapping layer.

It is also expected that the metal layer is formed on the surface of the base area shown in Fig. 4. This metal layer may trap quasiparticles excited in the base and the lifetime should be shorter than in the base under the junction area. However, when the electron beam irradiates position 1 in Fig. 7, the recombination in the base area is negligible, since the quasiparticles excited in the base need to diffuse out of the junction area to be trapped in the base metal layer. Contrarily, the quasiparticles excited in the counter are easily trapped in the counter metal layer because of short migration lengths of less than the thickness of the counter niobium. On the other hand, at position 2 the excited quasiparticles may be trapped in the base metal layer, but these quasiparticles cannot contribute to the decay curve. Only quasiparticles that diffuse into the junction area produce the junction signal, so that the decay curve reflects the quasiparticle lifetime in the base under the junction area.

The thermal quasiparticle density in niobium falls to $\sim 10^{12}$ cm^{-3} at 1 K and as low as ~ 1 cm^{-3} at 0.4 K, if the junction is ideal. This indicates that only self-recombinations take place in this temperature range, in which niobium junctions are normally operated for x-ray measurements. Namely, the quasiparticle recombination rate is determined by the density of excess quasiparticles created by x rays in place of the thermal quasiparticle density.[46] However, in reality all junctions possess a leakage current in some degree. As shown in Fig. 9, at 2.0 K the subgap current of the present junction is dominated by the tunneling current due to the thermal quasiparticles. On the other hand, the leakage current exceeds the quasiparticle tunneling current below 1.6 K, so that the subgap current is independent of temperature. Such leakage current may inject quasiparticles so that $N_{\rm th}$ in Eq. (4) is constant. If the constant values of b, $Z_1(0)$, and $N(0)$ are assumed, the quasiparticle lifetime is proportional to Δ^{-2}. This results in a 1.5 times longer τ_r^* in $R1$ than in the base. Thus, only the trapping effect could be responsible for the smaller counter signal to the x rays at 0.4 K.

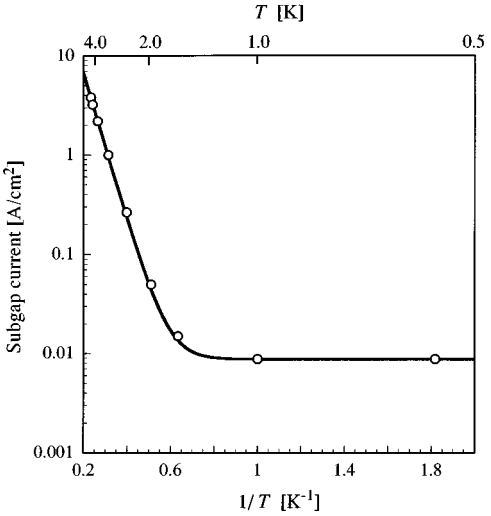

FIG. 9. Subgap current as a function of inverse temperature at a bias voltage of 0.6 mV. The solid line is the sum of the theoretical tunneling current due to the thermal quasiparticles and a leakage current of 0.0088 A/cm^2.

V. CONCLUSION

The LTSEM two-dimensional images have revealed that the base electrode of the polycrystalline Nb-Al/AlO_x-Nb junction produces a signal more than two or possibly four times larger than the counter. By the time decay measurements the effective quasiparticle lifetimes have determined: 100 ns in the counter and 280 ns in the base at 2.0 K. The effective lifetime in the base indicates that the phonon decay time is as short as 10 ps. It is implied that the 2Δ phonon decay is enhanced by a large factor at the grain boundaries in the polycrystalline niobium films.

The model structure has been proposed for the Δ spatial variation in consideration of the I-V characteristics and the measured quasiparticle lifetimes. The model structure involves the reduced-Δ regions due to the proximity effect. It is concluded that the causes of the asymmetric response to the electron beam are (1) the short quasiparticle lifetime in the counter electrode, (2) the small quasiparticle trapping effect due to the aluminum proximity layer in the base, and (3) the dominant trapping effect due to the proximity surface layer of the metallic oxide in the counter. The x-ray spectra are consistent with the above interpretation.

ACKNOWLEDGMENTS

The authors would like to express their thanks to S. Kiryu, S. Kohjiro, Y. Murayama, M. Maezawa, A. Shoji, M. Koyanagi, G. Linker, and J. Geerk for experimental assistance and fruitful discussions. M.O. is most grateful to O. Meyer for a guest position at FZK.

*Permanent address: Electrotechnical Laboratory, Umezono, Tsukuba, Ibaraki, 305, Japan. Electronic address: ohkubo@etl.go.jp.

†Present address: Universität zu Köln, Physikalisches Institut II, Lehrstuhl für Angewandte Physik, Zuelpicher Straβe 77, D-50937 Köln, Germany.

[1] M. Kurakado, Nucl. Instrum. Methods **196**, 275 (1982).

[2] N. Rando, A. Peacock, A. van Dordrecht, C. Foden, R. Engelhardt, B. G. Taylor, P. Gare, J. Lumley, and C. Pereira, Nucl. Instrum. Methods Phys. Res. A **313**, 173 (1992).
[3] P. Verhoeve, N. Rando, P. Videler, A. Peacock, A. van Dordrecht, D. J. Goldie, J. M. Lumley, J. Howlwtt, M. Wallis, and R. Venn, Proc. SPIE **2283**, 172 (1994).
[4] M. Kishimoto, M. Ukibe, M. Katagiri, M. Nakazawa, and M. Kurakado, Nucl. Instrum. Methods Phys. Res. A **370**, 126 (1996).
[5] A. Matsumura, T. Takahashi, and M. Kurakado, Nucl. Instrum. Methods Phys. Res. A **329**, 227 (1993).
[6] C. A. Mears, S. E. Labov, M. Frank, M. A. Lindeman, L. J. Hiller, H. Netel, and A. T. Barfknecht, Nucl. Instrum. Methods Phys. Res. A **370**, 53 (1996).
[7] M. Kurakado, Nucl. Instrum. Methods Phys. Res. A **314**, 252 (1992).
[8] D. V. Vechten and K. S. Wood, Phys. Rev. B **43**, 12 852 (1991).
[9] S. B. Kaplan, C. C. Chi, D. N. Langenberg, J. J. Chang, S. Jafarey, and D. J. Scalapino, Phys. Rev. B **14**, 4854 (1976).
[10] A. Rothwarf and B. N. Taylor, Phys. Rev. Lett. **19**, 27 (1967).
[11] F. Pröbst, H. Kraus, T. Peterreins, and F. V. Feilitzsch, Nucl. Instrum. Methods Phys. Res. A **280**, 251 (1989).
[12] M. G. Blamire, F. S. Porter, E. C. G. Kirk, and D. van Vechten, IEEE Trans. Appl. Supercond. **5**, 3014 (1995).
[13] N. Rando, A. Peacock, A. van Dordrecht, P. Hübner, P. Videler, J. Salmi, and I. Suni, J. Appl. Phys. **76**, 2490 (1994).
[14] D. Twerenbold and A. Zehnder, J. Appl. Phys. **61**, 1 (1987).
[15] H. Kraus, Th. Peterreins, F. Pröbst, F. van Feilitzsch, R. L. Mössbauer, and V. Zacek, Europhys. Lett. **1**, 161 (1986).
[16] J. Geerk, M. Gurvitch, D. B. McWhan, and J. M. Rowell, Physica B **109/110**, 1775 (1982).
[17] M. Kurakado, T. Takahashi, and A. Matsumura, Appl. Phys. Lett. **57**, 1933 (1990).
[18] S. Lemke, F. Hebrank, F. Fominaya, R. Gross, R. P. Huebener, N. Rando, A. van Dordrecht, P. Huebener, P. Videler, and A. Peacock, Physica B **194–196**, 1663 (1994).
[19] L. Y. Shen, in *Superconductivity in d- and f-Band Metals*, edited by D. H. Douglas, AIP Conf. Proc. No. 4 (AIP, New York, 1972), p. 31.
[20] J. Halbritter, Appl. Phys. A **43**, 1 (1987).
[21] F. S. Porter, D. van Vechten, M. G. Blamire, and E. C. G. Kirk, IEEE Trans. Appl. Supercond. **5**, 3026 (1995).
[22] J. Martin, S. Lemke, R. Gross, R. P. Huebener, P. Videler, N. Rando, T. Peacock, P. Verhoeve, and F. A. Jansen, Nucl. Instrum. Methods Phys. Res. A **370**, 88 (1996).
[23] S. P. Zhao, F. Finkbeiner, Ph. Lerch, A. Zehnder, and H. R. Ott, J. Low Temp. Phys. **93**, 641 (1993).
[24] R. Cristiano, L. Frunzio, R. Monaco, C. Nappi, and S. Pagano, Phys. Rev. B **49**, 429 (1994).
[25] R. P. Huebener, Rep. Prog. Phys. **47**, 175 (1984).
[26] R. Gross and D. Koelle, Rep. Prog. Phys. **57**, 651 (1994).
[27] L. Reimer, *Scanning Electron Microscopy* (Springer-Verlag, Heidelberg, 1985).
[28] V. Narayanamurti, R. C. Dynes, P. Hu, H. Smith, and W. F. Brinkman, Phys. Rev. B **18**, 6041 (1978).
[29] P. A. Warburton and M. G. Blamire, IEEE Trans. Appl. Supercond. **5**, 3022 (1995).
[30] A. D. Hahn, R. J. Gaitskell, N. E. Booth, and G. L. Salmon, J. Low. Temp. Phys. **93**, 611 (1993).
[31] S. B. Kaplan, J. Low Temp. Phys. **37**, 343 (1979).
[32] W. Eisenmenger, K. Laβmann, H. J. Trumpp, and R. Krauβ, Appl. Phys. **11**, 307 (1976).
[33] H. J. Maris and S. Tamura, Phys. Rev. B **47**, 727 (1993).
[34] S. Kominami, H. Yamada, N. Miyamoto, and K. Takagi, IEEE Trans. Appl. Supercond. **3**, 2182 (1993).
[35] N. Rando, P. Videler, A. Peacock, A. van Dordrecht, P. Verhoeve, R. Venn, A. C. Wright, and J. Lumley, J. Appl. Phys. **77**, 4099 (1995).
[36] K. E. Gray, Appl. Phys. Lett. **32**, 392 (1978).
[37] N. E. Booth, Appl. Phys. Lett. **50**, 293 (1987).
[38] D. J. Goldie, N. E. Booth, C. Patel, and G. L. Salmon, Phys. Rev. Lett. **64**, 954 (1990).
[39] R. Cristiano, E. Esposito, L. Frunzio, S. Pagano, L. Parlato, G. Peluso, G. Pepe, U. Scotti di Uccio, H. Nakagawa, M. Aoyagi, H. Akoh, and S. Takada, Appl. Phys. Lett. **67**, 3340 (1995).
[40] A. A. Golubov, E. P. Houwman, J. G. Gijsbertse, J. Flokstra, H. Rogalla, J. B. le Grand, and P. A. J. de Korte, Phys. Rev. B **49**, 12 953 (1994).
[41] K. Schwidtal, J. Appl. Phys. **43**, 202 (1972).
[42] W. DeSorbo, Phys. Rev. **132**, 107 (1963).
[43] C. C. Koch, J. O. Scarbrough, and D. M. Kroeger, Phys. Rev. B **9**, 888 (1974).
[44] G. Linker, Radiat. Eff. **47**, 225 (1980); (unpublished).
[45] A. Taylor and N. J. Doyle, J. Less-Common Met. **13**, 313 (1967).
[46] P. Verhoeve, N. Rando, J. Verveer, A. Peacock, A. van Dordrecht, P. Videler, M. Bavdaz, D. J. Goldie, T. Lederer, F. Scholze, G. Ulm, and R. Venn, Phys. Rev. B **53**, 809 (1996).